PRELIMINARY ASSESSMENT OF *PHELLINUS WEIRII* - INFECTED (LAMINATED ROOT ROT) TREES WITH HIGH RESOLUTION CASI IMAGERY

Donald G. Leckie[1], Cara Jay[2], Dennis Paradine[2] and Rona Sturrock[1]

[1] Canadian Forest Service, Pacific Forestry Centre
506 West Burnside Road, Victoria, B.C. V8Z 1M5

[2] MacMillan Bloedel Ltd.
65 Front Street, Nanaimo, B.C. V9R 5H9

ABSTRACT

Root diseases caused by several endemic fungi are economically and ecologically important disturbance agents in the forests of western North America. Laminated root rot (*Phellinus weirii*) has particularly important impact in coastal Douglas-fir stands. Forest managers would like an economical survey procedure for detecting pockets of *Phellinus weirii* infected trees for the purpose of salvage, remedial activities and inventory. Aerial survey with multispectral imagers such as casi, coupled with automated detection of damaged trees may provide a cost-effective survey method.

Casi imagery in eight spectral bands has been corrected to an orthoimage and radiometric corrections for the effects of illumination and view angle applied. Trees of varying levels of root rot symptoms were assessed in the field and related to delineated trees on the imagery. Visual symptoms on the ground ranged from subtle crown shape and growth rate changes, through gradual needle loss, to mortality. Chlorosis occurred on some trees. Preliminary analysis, including classification and regression analyses of symptom classes or levels, indicates that light crown symptoms will be difficult to consistently detect. However, moderate and severe damage including needle loss (e.g., > 25%) does appear to be detectable. Isolated trees of similar characteristics as root rot infected trees do appear on the imagery in scattered locations unrelated to root rot activity. It is anticipated that these false alarms can be largely mitigated by identifying the characteristic pattern of root rot damaged trees (i.e., stressed trees around a centre, the centre often being a hole or gap in the canopy).

Keywords: Phellinus, root rot, damage, remote sensing, casi, Douglas-fir.

RÉSUMÉ

ÉVALUATION PRÉLIMINAIRE D'ARBRES INFECTÉS PAR LA CARIE JAUNE ANNELÉE (*PHELLINUS WEIRII*) À L'AIDE DE L'IMAGERIE CASI À HAUTE RÉSOLUTION

Les maladies des racines causées par des champignons endémiques ont des effets perturbateurs importants sur les plans économique et écologique dans les forêts de l'ouest de l'Amérique du Nord. La carie jaune annelée (*Phellinus weirii*) a une incidence particulièrement grave sur les peuplements de Douglas verts. Les aménagistes aimeraient pouvoir appliquer une procédure peu coûteuse de reconnaissance pour détecter les poches d'arbres

Automated Interpretation of High Spatial Resolution Digital Imagery for Forestry. Victoria, British Columbia, Canada, February 10-12, 1998. D.A. Hill and D.G. Leckie, editors. Natural Resources Canada, Canadian Forest Service, Pacific Forestry Centre, Victoria, British Columbia. pp. 187-195.

infectés par le *Phellinus weirii* à des fins de récupération, de traitement et d'inventaire. Les levés aériens à l'aide de spectromètres imageurs comme le CASI, couplés à la détection automatisée des arbres endommagés pourraient constituer une méthode rentable.

L'imagerie CASI dans huit bandes spectrales a été transformée en orthoimage et corrigée au plan radiométrique pour compenser les effets de l'éclairement lumineux et de l'angle d'observation utilisé. Des arbres de hauteurs diverses ou présentant des symptômes de carie jaune annelée ont été évalués sur le terrain et associés à des arbres délimités sur l'imagerie. Les symptômes observés visuellement au sol comprenaient des changements subtils de la forme des houppiers et du taux de croissance, en passant par la perte graduelle des aiguilles et la mortalité. Certains arbres étaient atteints de chlorose. Une analyse préliminaire, comprenant des analyses de classification et de régression des classes ou des niveaux symptomatiques, indique que les symptômes associés au rétrécissement des houppiers seront difficiles à détecter de façon constante. Cependant, les dommages moyens et graves ainsi que la perte des aiguilles (soit > 25 %) semblent être détectables. Des arbres isolés présentant des caractéristiques similaires aux arbres infectés par la carie jaune annelée apparaissent sur l'imagerie en divers endroits, mais ne sont pas associés aux infections par la carie jaune annelée. Nous croyons que ces fausses alarmes peuvent être atténuées en identifiant le modèle caractéristique des arbres atteints par la carie jaune annelée (c'est-à-dire des arbres soumis à un stress autour d'un point, le point étant souvent une trouée dans le couvert forestier).

INTRODUCTION

Root diseases are becoming increasingly important damage agents in the forests of northwestern North America. Laminated root rot (LRR) is the most important single natural disturbance causing long-term change in these forest ecosystems (Thies, 1998). LRR impacts forest productivity by reducing tree growth and by killing trees. *Phellinus weirii* (Murr.) Gilbn., the causal organism, is a native fungal pathogen which has coevolved with native coniferous species such as its principle host, Douglas-fir (*Pseudotsuga menziesii* (Mirb.) Franco. Other susceptible hosts include true firs (*Abies* spp.) and mountain and western hemlock (*Tsuga mertensiana* (Bong.) Carr. and *Tsuga heterophylla* (Raf.) Sarg.). Resistant hosts include western redcedar (*Thuja plicata* Donn ex D. Don). All hardwoods are immune to *P. weirii* infection.

The disease begins in a stand when uninfected roots of a susceptible tree contact infected stumps or roots (i.e., inoculum) left from a previous stand. Inoculum of *P. weirii* can survive in large infected stumps and roots for 50 years or longer. Once established in the roots of a susceptible host, *P. weirii* progressively causes decay, resulting in reduced uptake of water and nutrients and weakened structural support to infected roots (Thies and Sturrock, 1995). Trees of all ages are susceptible to *P. weirii* infection, although older trees are better able to withstand the damaging effects. As with other root pathogens, the damage that *P. weirii* causes to roots underground is eventually expressed above-ground in the crown. Crown symptoms caused by *P. weirii* usually develop only after the fungus has killed and decayed a significant portion of the root system. In young stands, trees growing near inoculum may develop crown symptoms and be killed within a few years of infection. In older stands, crown symptoms may appear 5 to 15 years after initial infection. Larger infected trees may live for decades after symptoms first appear, with progressively more severe symptoms and concurrent growth loss (Thies and Sturrock, 1995). Crown symptoms caused by *P. weirii* and visible from the ground include the following:

- reduced height growth in branches but especially evident in the leader; trees in decline for many years develop a rounded or dome-shaped top with crowns eventually dying
- needle chlorosis
- needle loss
- production of large numbers of stress-induced, smallish cones. Mortality can eventually occur.

Stand level symptoms evident on the ground and from the air include canopy openings which have standing dead trees, windthrown trees and crown symptomatic trees at their edges. These centres of infection expand approximately radially at about 30 cm per year (Thies and Sturrock, 1995). In coastal areas of the Pacific Northwest, patches of hardwoods such as red alder (*Alnus rubra* Bong.) often develop in LRR centres.

Information on the location and quantity of root disease is important for management planning, for inventory to assess the impact on wood supply, for salvage logging and for planning remedial activities such as stump removal and planting of non-susceptible species. It is often highly desirable to log affected trees before they lose value. The operational forester's main requirement is the detection of infected areas and individual pockets. The forester will generally follow up with site visits before executing or planning an operation. There is therefore a fairly high tolerance of false alarms. Quantification of the root disease is beneficial, but not a high priority. There are often large areas of susceptible forest, but the target (infected areas) is small, sometimes just a few trees. Effective ground surveys for detection of root rot are therefore difficult. They are time consuming, require specialized expertise and are expensive. Recent surveys in coastal B.C. have cost $40 to $70/ha (personal communication D. Clark, G. Fournier). A cost-effective aerial survey method would be valuable.

This study assesses the potential of automated classification methods applied to high resolution airborne multispectral imagery (casi) for assessing the level of root rot on an individual tree basis in order to detect, map and quantify laminated root rot occurrences. This investigation is complementary with an independent study (Reich and Price, 1998) examining high resolution casi data for Tomentosus root disease damage of spruce in the interior of British Columbia.

DATA

Imagery was acquired with the casi imaging spectrometer (Anger at al., 1994) over a test area near Nanaimo, British Columbia, Canada (49° 06' N; 124° 00' W). Two adjacent flight lines were flown September 27, 1996. The area is on the east coast of Vancouver Island within the Coastal Douglas-fir moist maritime biogeoclimatic zone. It is predominated by second growth stands of Douglas-fir aged 75 to 85 years with heights ranging from 30 to 35 m. Stands regenerated following clearcutting and have undergone varying degrees of thinning.

Data resolution is 60 cm and consists of eight spectral bands at 438 nm, 489 nm, 550 nm, 601 nm, 656 nm, 715 nm, 795 nm and 861 nm with approximately 25 nm bandwidths. Data from only one of the flight lines was used for this study. It should also be noted that similar data was acquired in November, 1995 and will be examined in subsequent analyses. Data was geometrically corrected to cartographic coordinates by Itres Research Ltd.

The data was radiometrically adjusted to take into account the effect of varying illumination and view angle conditions (i.e., the bidirectional reflectance distribution function, BRDF). Trees were automatically isolated with the valley following approach described by Gougeon (1998). A preliminary broad cover type classification of the isolated trees to identify conifer trees was then conducted. The mean value in each spectral band, derived from all pixels within the isolated tree, was taken to represent the signature for that tree. The average, within each column, of all pixels classified as conifer was plotted and a third order polynomial fit to these points (Figure 1). This created a correction curve for each band. A correction (offset) was then applied to the pixel values of each column of the image based on this correction curve. The offset was equal to the difference between the curve at that column and the curve at nadir. The mean value of trees in each column of the resulting corrected image should, therefore, all be approximately equal to the mean value at nadir. In other applications of this technique an iterative procedure is used. After the correction described above, a second classification of conifers is conducted using the corrected data, a new correction curve generated and applied. This is necessary when significant errors in the initial conifer classification occur due to the BRDF effect present in the original imagery. This additional step was unnecessary with the image used in this study. Another unique feature of the correction system is that it can be applied to geometrically corrected imagery. The imagery in essence is realigned along its edges to approximate the original column oriented non-geometrically corrected imagery.

A specialized ground survey was conducted to define root disease conditions in the study area. Sites of suspected or known laminated root rot were visited. Trees in the immediate vicinity of root disease centres and trees some distance away from centres were numbered and located on hardcopy casi images. Five sites were selected and 260 trees marked and assessed. Species, dbh and dominance were recorded for each tree. The crowns of most trees were photographed.

A) percent needle loss	estimated to nearest 5%	
B) chlorosis	N	nil
	?	colouration may be a little abnormal but not definite
	L	light chlorosis
	M	moderate chlorosis
	S	severe chlorosis
C) crown health class	1)	Healthy (full crown, good leader and shoot growth, conical crown, no discolouration)
	2)	Lightly Symptomatic (reduction in shoot length; crown may be rounded, there may be slight chlorosis; little or no foliage loss or crown thinning)
	3)	Moderately Symptomatic (may have reduction in shoot length and rounded crown, may be chlorotic, has foliage loss and thinning of the crown foliage)
	4)	Severely Symptomatic (reduction in shoot length, usually with rounded crown, may be chlorotic, foliage loss and crown thinning is large)
	5)	Dead (100% needles loss, most branches still intact)
		Gradations were also included between classes.

Table 1. Crown conditions assessed in the ground survey of root disease symptoms.

An independent (i.e., without access to the casi imagery) assessment of the root disease condition of each of the 260 trees was conducted by experts. Three aspects of crown symptoms were assessed: percent needle loss, chlorosis level, and crown health class. Table 1 gives details of these assessments. Crown health class incorporated, in an overall assessment, needle loss, chlorosis, shoot length reduction and rounding of crown shape. It was adapted from a similar system of Reich and Price (1998) used for assessing Tomentosus root disease. There were few trees with signs of chlorosis in the test sites. Finally, an overall assessment of whether a tree was affected by laminated root rot was also made taking into account all available field observations. Special features of the tree that might influence its spectral characteristics were also coded on the field sheet. These include whether the trees were large, open-grown, or edge trees (i.e., at the edge of an opening). The authors have observed in other studies that such trees often have 'abnormal' spectral signatures due to more of the crown being exposed to illumination of direct sunlight. Trees judged to be exceptionally healthy and vigorous trees were noted. Snags were also recorded as was their degree of branch loss. Snags were differentiated from newly dead trees with most of their fine branching remaining and the latter were designated as having 100% needle loss. Regression analyses of band intensity values versus percent needle loss included only these 100% needle loss trees (not the snags).

DATA ANALYSIS, RESULTS AND DISCUSSION

Trees were manually delineated on the casi imagery and the multispectral signature for each tree was generated. This signature included the mean value in each spectral band for all the pixels within the outlined area of the tree. These were used in subsequent regression analysis and test classification.

The mean value for each tree was plotted against both needle loss and crown health class. Relationships were curvilinear for crown health class. This is to be expected as the classes are gradational with only small changes in symptoms for the light classes; these mostly being represented by changes in shoot length and crown form which may have little effect on spectral reflectance. Figure 2 shows the relationship of band intensity versus percent needle loss for selected bands. The relationship is linear. Table 2 gives the linear correlation coefficient for each band. It can be seen that the 550 nm, 601 nm and 715 nm bands had poor capabilities for differentiating damage levels; the 438 nm, 489 nm, 656 nm, 795 nm and 861 nm bands had moderate relationships. The 656 nm band had the highest correlation, followed by the blue and then near-infrared bands. Ratios of bands were also investigated (Figure 2; Table 2). The ratios improved the relationships. NDVI (795 nm - 656 nm)/(795 nm + 656 nm) proved the best with an r^2 of 0.84; the red over green band ratio (656 nm)/(550 nm) was also good.

Bands (nm)	r^2	Band Ratios (nm)	r^2
438	0.33	795/656	0.68
489	0.32	795/550	0.68
550	0.05	795/489	0.71
601	0.19	656/550	0.78
656	0.38	656/489	0.26
715	0.00	(795-656)/(795+656)	0.84
795	0.28	-	-
861	0.26	-	-

Table 2. Correlation coefficients of band intensity versus percent needle loss.

Because of the limited number of ground truthed trees examined in this preliminary study, a test classification of the manually delineated trees was conducted using all trees to generate the class signatures. Each tree contributes one value (mean of all pixels) for each band. Classes were healthy, light, moderate, severe and dead. The classes were based on crown health class. Dead consisted of 100% defoliated trees, but no snags. A maximum likelihood classification was then conducted on the trees using all bands except the 438 nm band which was somewhat noisy. Figure 3 gives the classification results and the ground truth tree classes for comparison. For the 73 trees tested, accuracy was 77% overall by individual tree and 88% by class average. Results should be treated with caution as they are the same trees as were used to generate the classification signatures. Dead, severe and moderate classes had little confusion, but light and healthy were confused by 12 to 27%. Some light and healthy trees were classified as moderate (7 % and 13%, respectively).

To get a better indication of expected results for operational surveys the classification was conducted on automatically isolated tree crowns. The signatures from the manually delineated trees were used to represent the classes. The trees were isolated using a valley following approach (Gougeon, 1998). Figure 4 gives the results for a segment of the flight line. Several zones of damaged trees are evident. Reconnaissance inspection of these sites indicated that many were associated with root disease, however, others may be related to other possible stresses. Isolated trees of light and to a lesser extent moderate damage are scattered within the image segment. Again, a sample of trees were checked and some were found to be affected by root disease, while others did not appear to be.

Results suggest that there may be quite a few spurious trees identified as the light damage class and using the light class on its own as a root rot indicator may result in too many false alarms. However, the characteristic pattern of damage will be useful for narrowing the zones and trees that potentially have root disease. This pattern consists of affected trees concentrating about a centre (the centre often being an opening in the canopy) with the severity of tree symptoms decreasing away from the centre. Visual scanning of the single tree classification results would be a simple procedure for identifying likely root disease centres and eliminating some false alarms. With further development, automated procedures to utilize this pattern could be created. Foresters are willing to accept a fair number of false alarms; the importance of not missing an infected area is high. Therefore, it may not be desirable to try to eliminate too many lightly affected trees in the classification. As well, accurate quantification of the level of damage on a trees basis is often not mandatory; it is the presence and location of a root rot centre and its size or number of affected trees that is important.

When applied with the single tree isolation algorithm some additional problems occur. Several trees may be combined into one tree or a single large tree broken into more than one crown. Both these types of errors can result in poor classifications of those crowns. As well, the isolation routine because it is based on outlining bright areas around darker (shaded) areas, can create "trees" in non-forest areas. A spectral classification prior to or after the isolation is used to eliminate these as much as possible. This was done in this study. A general conifer tree class separated most healthy and damaged trees from other non-tree isolated features. However, the spectral characteristics of some severely damaged trees were similar to various non-tree isolated areas. It was difficult to separate these areas from severely damaged trees without also eliminating the damaged trees.

Erroneous damaged trees therefore may appear in open areas. Again, this problem may be resolved simply by visual inspection or more sophisticated techniques, but it does demonstrate some of the considerations for operational use of the methods described above.

Further work will involve view/illumination angle (BRDF) correction of the second flight line of casi data and radiometric normalization to the data used in this paper. The data of the two lines can then be analyzed together and all the field sites used. Further testing with the automatically isolated trees and the 1995 casi data is in order. The quantitative accuracy will be tested, but a key parameter will be the degree of false alarms generated and, of course, acceptance of the methods by the operational forester as a potential useful and viable tool.

CONCLUSIONS

Results of this study are promising in terms of identifying trees moderately or severely affected by root disease with automated isolation and classification techniques applied to high resolution casi or similar multispectral imagery. Dead trees are also well differentiated. There are spectral differences in the 438 nm, 489nm, 656 nm, 795 nm and 861 nm bands. Ratios of bands were notably better than the single bands, in particular an NDVI and 656 nm/550 nm ratio. With the data tested, moderate and severe symptoms had good detection. Light crown symptoms may, however, be difficult to consistently detect. There may be considerable numbers of false alarms in terms of scattered trees identified as infected. It is anticipated the false alarms can be mitigated by using the pattern of damaged trees characteristic of root disease centres, either visually or in an automated procedure. Further testing is needed to prove the results and test the viability of the methods.

ACKNOWLEDGEMENTS

The study is part of a larger cooperative project of Macmillan Bloedel Ltd., Itres Research Ltd. and the Canadian Forest Service (Pacific Forestry Centre) entitled "Development of Certified Forestry Applications Using Compact Spectrographic Imager (casi) Data". The project is sponsored and funded by Forest Renewal British Columbia. The authors thank Bill Schuckel of Macmillan Bloedel Ltd., South Island Division for supporting and providing information for the study. Itres Research Ltd. acquired and geometrically corrected the imagery. Dr. François Gougeon of the Pacific Forestry Centre provided valuable assistance in tree isolation and development of BRDF correction procedures.

REFERENCES

Anger, C.D., S. Mah, and S.K. Babey. 1994. Technological enhancements to the compact airborne spectrographic imager (casi). *Proc. 1st Int'l Airborne Remote Sensing Conference and Exhibition.* September, Strasbourg, France. Vol. II, pp. 205-213.

Gougeon, F.A. 1998. Automatic individual tree crown delineation using a valley-following algorithm and rule-based system. *Proc. Int'l Forum on Automated Interpretation of High Spatial Resolution Digital Imagery for Forestry.* February, Victoria, B.C., Canada.

Reich, R.W. and R. Price. 1998. Detection and classification of forest damage caused by Tomentosus root rot using an airborne multispectral imager (casi). *Proc. Int'l Forum on Automated Interpretation of High Spatial Resolution Digital Imagery for Forestry.* February, Victoria, British Columbia, Canada.

Thies, W.G. and R.N. Sturrock. 1995. Laminated root rot in western North America. General Technical Report PMW-349, U.S. Dept. Agriculture, Forest Service.

Thies, W.G. 1998. Laminated root rot. *In* Compendium of Conifer Diseases, E.M. Hansen and K.J. Lewis, Editors, APS Press, St. Paul, Minnesota. pp. 14-15.

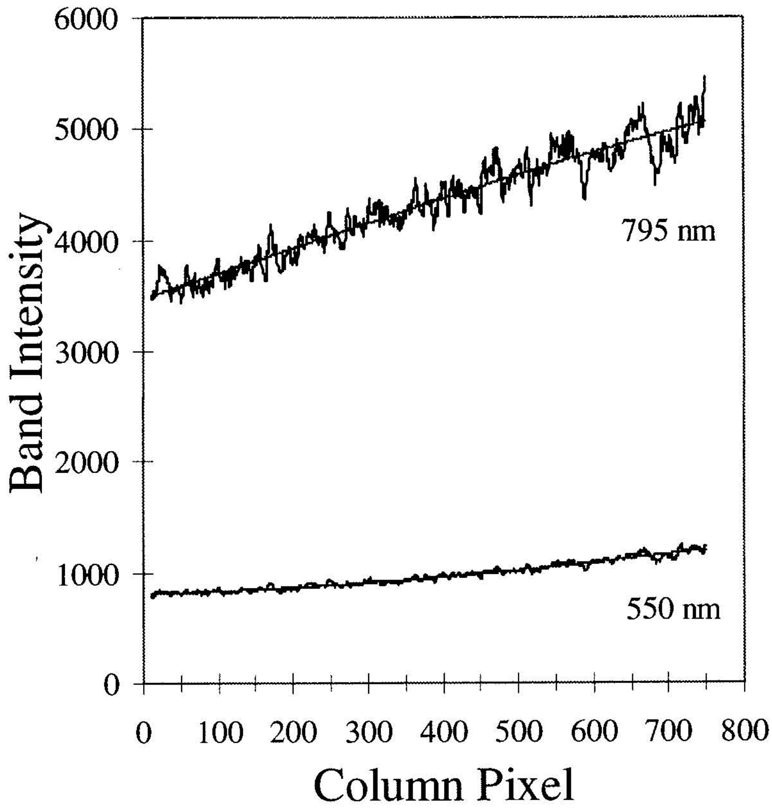

Figure 1. Combined effects of illumination, view angle, and atmospheric conditions on the imagery. The column average of pixel values under a mask representing the automatically delineated conifer trees are plotted along with a third order polynomial correction curve fitting these data.

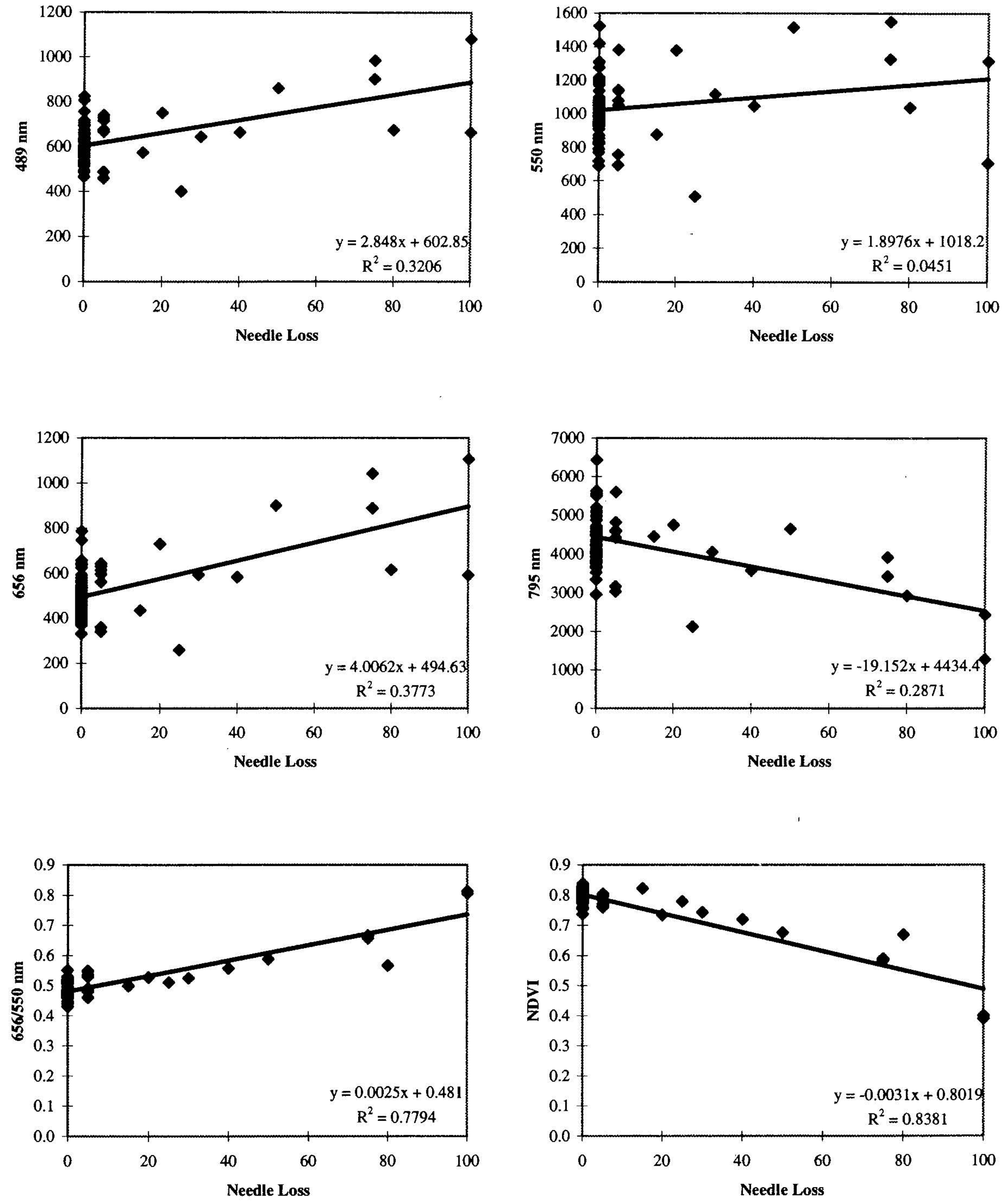

Figure 2. Band intensity versus percent needle loss for ground truth trees with a straight-line regression fit plotted.

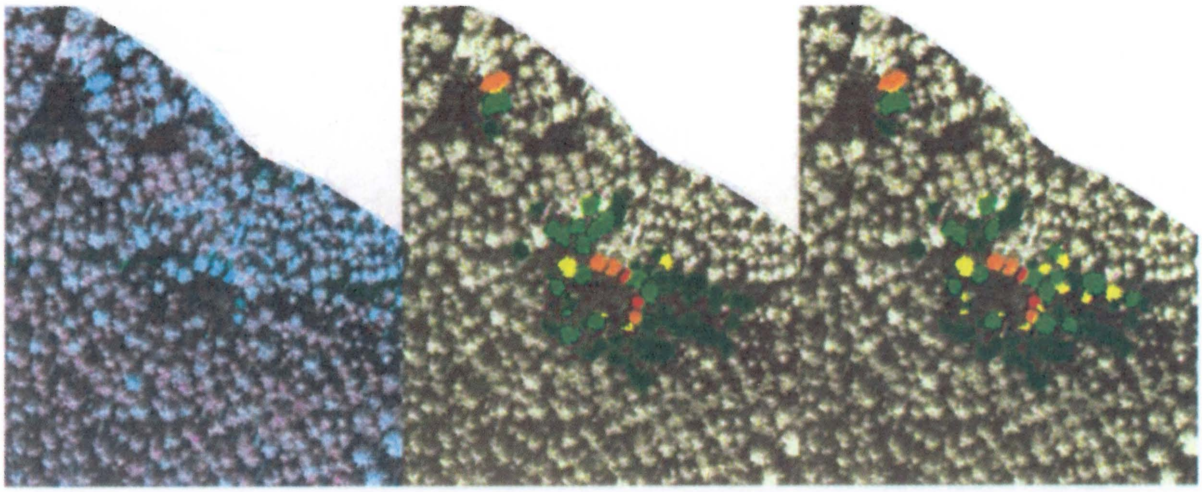

a) b) c)

Figure 3. Classification results for ground truth trees. a) colour infrared band combination, b) ground truth trees manually delineated and ground truth class colour coded (healthy = dark green; light = light green; moderate = yellow; severe = orange; dead = red), c) classification results for ground truth trees.

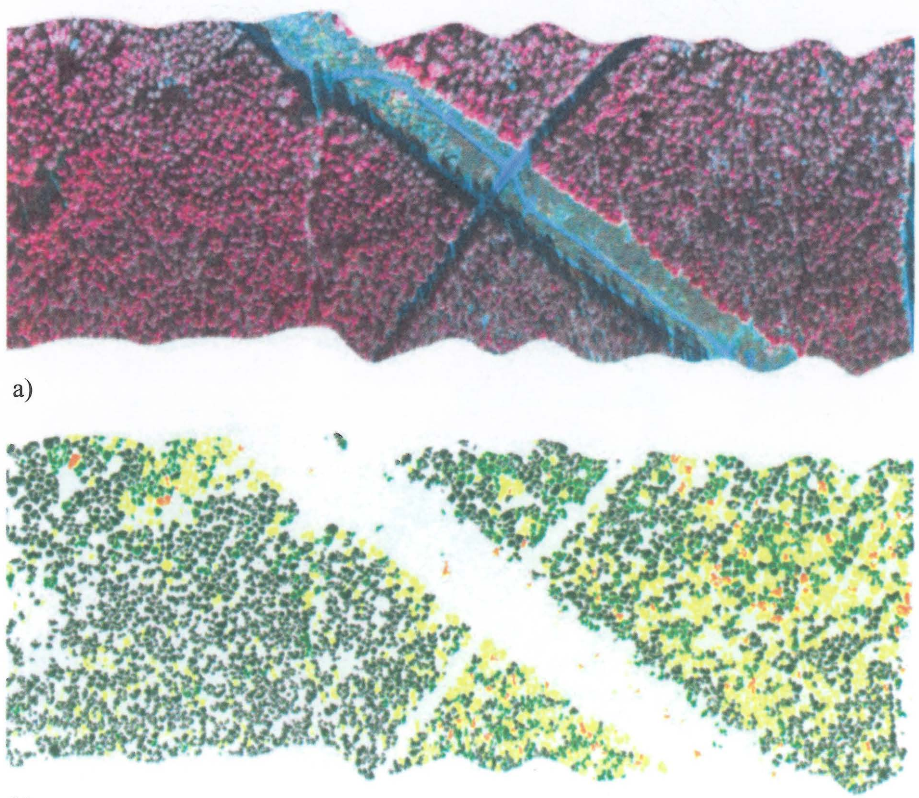

a)

b)

Figure 4. Classification results on automatically isolated trees for an approximately 750 m long image segment. (dark green = healthy; light green = light; yellow = moderate; orange = severe; red = dead)